Maekawa K, Saeki M, Saito Y, Ozawa S, Kurose K, Kaniwa N, Kawamoto M, Kamatani N, Kato K, Hamaguchi T, Yamada Y, Shirao K, Yasuhiro S, Muto M, Doi T, Ohtsu A, Yoshida T, Matsumura Y, Saijo N, Sawada J.	Genetic variations and haplotype structures of the DPYD gene encoding dihydropyrimidine dehydrogenase in Japanese and their ethnic differences	Journal of Human Genetics	52	804-819	2007
Wang L, Kuwahara Y, Li L, Baba T, Shin RW, Ohkubo Y, Ono K, Fukumoto M.	Analysis of common deletion (CD) and a novel deletion of mitochondrial DNA induced by ionizing radiation	International Journal of Radiation Biology	83	433-442	2007
Roudkenar YH, Kuwahara Y, Baba T, Roushandeh AM, Ebishima S, Abe S, Ohkubo Y, Fukumoto M.	Oxidative stress induced lipocalin 2 gene expression: Addressing its expression under the harmful conditions	Journal of Radiation Research	48	39-44	2007
Roudkenar M, Li L, Baba T, Kuwahara Y, Nakagawa H, Wang L, Kasaoka S, Ohkubo Y, Ono K, Fukumoto M.	Gene expression profiles in mouse liver cells after exposure to different types of radiation	Journal of Radiation Research	49	29-40	2008
Adbelwahab SA, Owada Y, Kitanaka N, Adida A, Sakagami H, Ono M, Watanabe M, Spener F, Kondo H.	Enhanced expression of adipocyte-type fatty acid binding protein in murine lymphocytes in response to dexamethasone treatment	Molecular and Cellular Biochemistry	299	99-107	2007

Nakamura K, Hirai H, Torashima T, Miyazaki T, Tsurui H, Xiu Y, Ohtsuji M, Lin QS, Tsukamoto K, Nishimura H, Ono M, Watanabe M, Hirose S.	CD3 and immunoglobulin G Fc receptor regulate cerebellar functions	Molecular and Cellular Biology	27	5128-5134	2007
Hishinuma T, Suzuki K, Saito M, Yamaguchi H, Suzuki N, Tomioka Y, Kaneko I, Ono M, GOto J.	Simultaneous quantification of seven prostanoids using liquid chromatography/tandem mass spectrometry: The effects of aarachidonic acid on prostanoid production in mouse bone marrow-derived mast cells	Prostaglandins, Leukotrienes and Essential Fatty Acids	76	321-329	2007
K Nakatani, W-M Qu, M-C Zhang, H Fujii, H Furukawa, T Miyazaki, M Iwano, Y Saito, M Nose, Masao Ono	A genetic locus controlling aging-sensitive regression of B lymphopoiesis in an autoimmune-prone MRL/lpr strain of mice	Scandinavian Journal Immunology	66	654-661	2007
Aoi A, Watanabe Y, Takahashi M, Mori S, Vassaux G, Kodama T.	Herpes simplex virus thymidine kinase-mediated suicide gene therapy using nano/microbubbles	Ultrasound in Medicine and Biology	34	425-434	2008
小玉　哲也	ナノ・マイクロバブルと超音波を用いた分子導入システムの開発とがん治療への応用	日本機械学会誌	111	51-54	2008.1

研究成果の刊行物・別刷

CONCISE REPORT

A non-major histocompatibility locus determines tissue specificity in the pathogenic process underlying synovial proliferation in a mouse arthropathy model

Ming-Cai Zhang, Shiro Mori, Fumiko Date, Hiroshi Furukawa, Masao Ono

Ann Rheum Dis 2007;**66**:242–245. doi: 10.1136/ard.2006.054999

Background: The incidence and characteristics of spontaneous ankylosis in the ankle of specific F_1 mice descended from two *Fas*-deficient strains were reported. Here the coincidence of synovial proliferation and ankylosis in the descendent F_2 mice is reported.
Aim: To clarify whether the two distinct manifestations are genetically different.
Methods: An arthropathic group of mice (MCF_2) were bred by intercrossing MRL/Mp.*Fas*^{lpr}-*sap*$^{-}$/*sap*$^{-}$ and C3H/He.*Fas*^{lpr} mice. All mice were killed by bleeding under anaesthesia when they were 6 months old. Pathological grades for synovial proliferation were determined by microscopical examination. To obtain a linkage locus, the whole genome of male MCF_2 mice was scanned by using 73 microsatellite markers.
Results: Synovial proliferation was equally observed in male and female MCF_2 mice. No correlation was observed between the grades of synovial proliferation and the ankylosis occurring in the MCF_2 mice. A suggestive susceptibility locus was shown in the middle of chromosome 11. This locus was an MRL allele with a recessive inheritance mode.
Conclusion: The pathogenic mechanisms of synovial proliferation and ankylosis are genetically different. The present locus is overlapped with some loci associated with rheumatoid arthritis and with others associated with experimental arthritides.

An inflammatory joint disease is usually recognised as an admixture of destruction and proliferation of the joint components. An imbalance of such counterprocesses may result in a pathological remodelling of joint structures giving rise to a unique clinicopathological outcome of the disease. Rheumatoid arthritis is characterised by synovial proliferation and erosion of joint cartilage due to chronic inflammation. The remodelling process in rheumatoid arthritis is associated with the contraction and destruction of joints. On the other hand, an ankylosing disease, another type of inflammatory joint disease, involves a distinct remodelling process causing joint ankylosis. Although the remodelling process for ankylosis has not been completely characterised, recent studies using rodent ankylosis models have evaluated the pathological proliferation of a particular region, where a joint capsule or ligament attaches to a bone.[1–4] The histological characteristics are proliferation, cartilage formation and, subsequently, replacement of cartilage by bone, a process typical of endochondral bone formation. The process is called ankylosing enthesitis. A comparative study on the distinct joint remodelling processes may shed new light on the distinct and essential mechanisms of rheumatoid arthritis and ankylosing diseases.

We recently reported a mouse model with spontaneous and male-predominant onset of progressive ankylosis in ankle joints.[5] It should be noted that this joint ankylosis occurred in a particular F_1 generation of mice, which descended from two ankylosis-free strains—MRL/Mp.*Fas*^{lpr}-*sap*$^{-}$/*sap*$^{-}$ (previously denoted as MRL/rpl)[6] and C3H/He.*Fas*^{lpr} (C3H/lpr). The MRL/rpl strain spontaneously arose from a lupus-prone MRL/Mp.*Fas*^{lpr} (MRL/lpr) strain. It is noteworthy that the mutation on signalling lymphocyte activation molecule (SLAM)-associated protein (SAP) attenuated the development of autoimmune diseases as seen in MRL/Mp.*Fas*^{lpr} (MRL/lpr) mice.[6] These mice develop spontaneous arthritis characterised by synovial proliferation; therefore, they are considered as a model for rheumatoid arthritis. The onset of ankylosis in (MRL/rpl×C3H/lpr) F_1 mice was unexpected. A defect of SAP or a coupling of two predisposed genes descended from the two parental strains was a possible interpretation for this onset. To deal with this issue, we performed a linkage analysis using (MRL/rpl × C3H/lpr) F_2 (MCF_2) mice and arrived at two genetic mechanisms for the onset of ankylosis in these mice: the dissociation of the SAP defect and association of the single locus on chromosome 7 with the onset of ankylosis.[5] Although the question is not completely answered, the results provided an opportunity to characterise a non-major histocompatibility complex (MHC)-linked locus associated with the pathogenesis of ankylosis.

In this study, we observed sporadic incidences of synovial proliferation and ankylosis (entheseal proliferation) in MCF_2 mice. The relationship between the pathogenic mechanisms of synovial and entheseal proliferations has been discussed. We provide evidence that the two distinct joint manifestations independently develop and are controlled differently by distinct genetic loci.

METHODS

Mice

C3H/lpr mice were purchased from The Jackson Laboratory (Bar Harbor, Maine, USA) and bred under specific pathogen-free conditions in the Animal Research Institute, Tohoku University Graduate School of Medicine, Sendai, Japan. MRL/rpl, MCF_1 and MCF_2 mice were housed in the same condition. In all animal experiments, we observed the Tohoku University guidelines for animal experimentation.

Histopathological grading of ankylosis

All mice were killed at 6-months of age under ether anaesthesia. Ankle joints were fixed in 10% formalin buffered with 0.01 M phosphate (pH 7.2), decalcified in 5% formic acid and 5% formalin and embedded in paraffin wax. Tissue sections were stained with haematoxylin and eosin. The pathological grade of the synovial proliferation was determined according to the following criteria: normal (grade 0), multiplication of synovial lining layer (grade 1) and grade 1 with villous

Abbreviations: MCF_2, (MRL/rpl×C3H/lpr)F_2; SAP, signalling lymphocyte activation molecule-associated protein; SLAM, signalling lymphocyte activation molecule

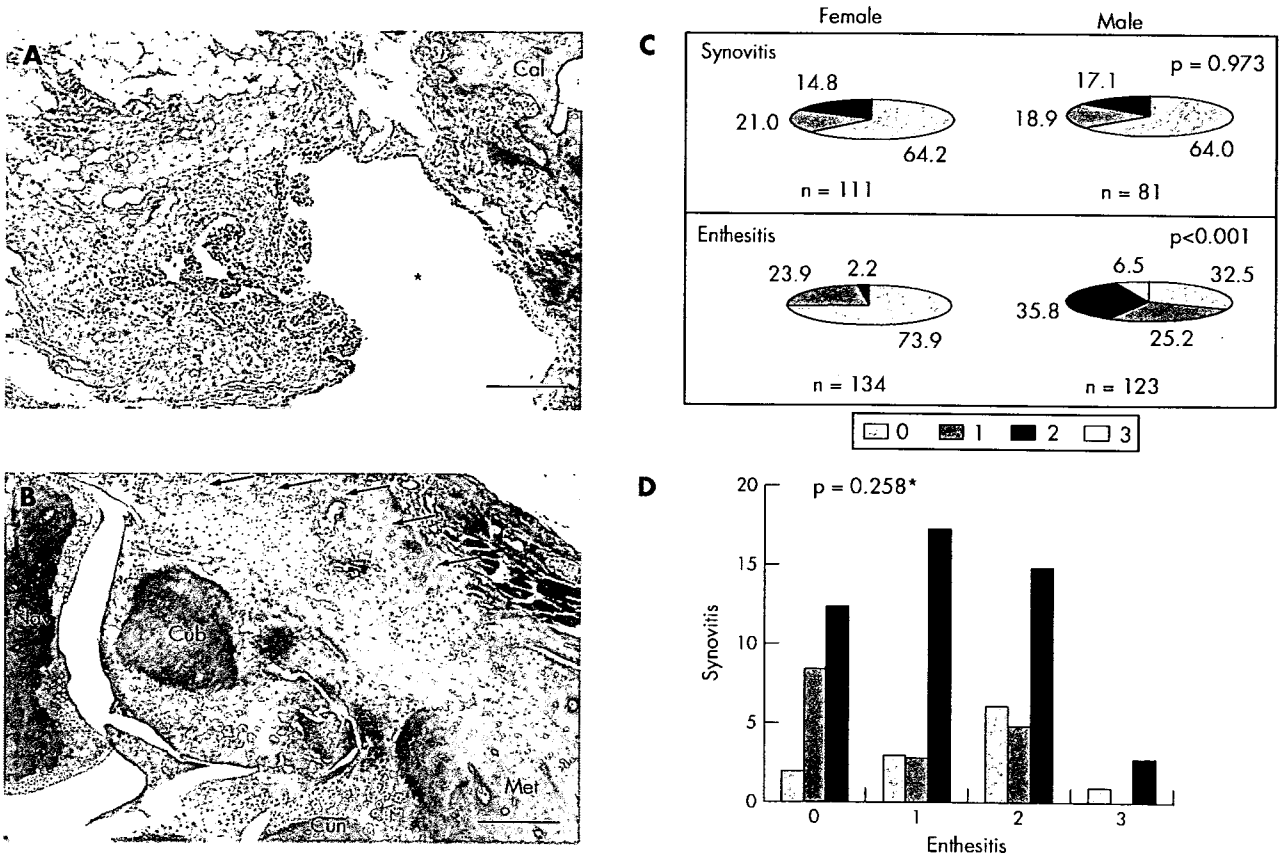

Figure 1 Specific manifestations of the synovitis or enthesitis developed in MCF_2 mice. Representative microscopic manifestations of synovitis (A) and enthesitis (B) in aged MCF_2 mice. Asterisk in (A) indicates a synovial cavity; arrows in (B) indicate the entheseal proliferation of ankle-associated tendon sheath (haematoxylin and eosin). Bars indicate 200 μm. (C) Percentage distribution of grades of synovitis and enthesitis in aged MCF_2 mice. The number of the mice analysed and p values provided by the χ^2 test are indicated. (D) The bar graph indicates the number distribution of grades of enthesitis and synovitis in the 81 male MCF_2 mice. No correlation is shown between the onsets of synovitis and enthesitis. p Value was determined by Fisher's exact test with standard 3×4 contingency matrices. Cub, cuboidal bone; Met, metatarsal bone; Nav, navicular bone; Cal, calcaneus; Cun, cuneiform bone.

proliferation (grade 2). The grade of an individual mouse was defined as a maximal grade determined in six longitudinal sections of bilateral hind paws. Samples inappropriate for microscopical examination, mainly because of the absence of synovium in accountable sections, were precluded from further analysis. The number of female and male MCF_2 mice accounted in this study was 111 and 81, respectively. The grade of ankylosis was determined previously.[5]

Genomewide screening for susceptibility loci to synovial proliferation

We searched association loci in the whole genome using 81 male MCF_2 mice and 73 microsatellite markers, which were all able to distinguish the parental genotypes and provided a coverage of the mouse genome with an average distance of 23.3 cM apart. The genetic positions of microsatellite markers and genes were determined on the basis of the Mouse Genome Informatics provided by The Jackson Laboratory.

Statistical analysis

A correlation between the grades of synovial proliferation and ankylosis was evaluated by Fisher's exact test with standard 3×4 contingency matrices. An association of the onset of synovial proliferation and the genotype at each marker position was evaluated by the χ^2 test with standard 2×3 contingency matrices. A significant or suggestive association was estimated by $p<0.000052$ or 0.0016, respectively, as recommended by Lander and Kruglyak.[7]

Table 1 Association of microsatellite genotype and the incidence of synovitis in MCF_2 male mice

		Incidence of synovitis							
	Position	Negative			Positive				
Marker	(CM)	MM	MC	CC	MM	MC	CC	χ^2 test	p Value
D11Mit71	1.1	13	25	14	7	16	6	0.48	0.79
D11Mit263	55.6	9	32	11	17	8	4	14.8	0.001
D11Mit334	68	11	29	12	12	13	4	3.92	0.14
D11Mit338	75	10	30	12	11	12	6	3.51	0.17

Genotypes *MM*, *MC* and *CC* indicate MRL/MRL homozygote, MRL/C3H heterozygote and C3H/C3H homozygote, respectively.

RESULTS

Incidence of synovial proliferation

In addition to the onset of ankylosis, we observed a thickening of the synovial lining layer, with mild lymphocytic infiltration and proliferation of small vessels in MCF_2 mice (fig 1A,B). Villous formations were evident in the advanced stage of the synovial proliferation. Neither lymphoid aggregation in the synovial lesion nor bone erosion with pannus-like formation was detected in all the mice examined. The microscopical incidence of synovial proliferation was 12/25 (48%) in MRL/rpl, 12/26 (46.2%) in C3H/lpr, 14/69 (20.3%) in MCF_1 and 69/192 (35.9%) in MCF_2 mice. The synovial lesion was detected equally in male and female MCF_2 mice ($p = 0.973$) (fig 1C). No significant correlation was obtained between the progression of ankylosis and synovial proliferation in male-only ($p = 0.258$, fig 1D) and all MCF_2 mice (data not shown).

Mapping of susceptibility loci associated with synovial proliferation

In this mapping study, we analysed the same MCF_2 mice that were used in the previous mapping study on ankylosis. The genomewide search using 81 male mice suggested a single marker *D11Mit263* (55.6 cM) on chromosome 11 that was significantly associated with the onset of synovial proliferation ($p<0.001$; table 1). The incidence of synovial proliferation in the MRL homozygote group (17/26, 65.4%) in association with *D11Mit263* was higher than that in the MRL/C3H heterozygote (8/40, 20%) and C3H homozygote (4/15, 26.7%) groups. This indicates that this MRL-derived locus regulates the onset of synovial proliferation in a recessive inheritance manner. No significant association was observed between synovial proliferation and any marker on the X chromosome where the SAP gene exists.

DISCUSSION

Recent studies have reported several mouse models with spontaneous ankylosis. DBA/1 is a spontaneous ankylosis model and an induced synovitis model with immunisation of type II collagen. The two DBA/1-related arthopathies develop similarly in a male-predominant fashion, although they are histopathologically different. It has been of particular interest to determine whether the pathogenic mechanisms of the distinct arthropathies in the DBA/1 mice are overlapped.

A cross mating of the DBA/1 strain with a particular lupus-prone strain such as BXSB or MRL/Mp resulted in an acceleration of the onset and increase in the severity of ankylosis in F_1 mice.[2 4] These facts may suggest a correlation between lupus susceptibility and the pathogenesis of ankylosis. The MCF_2 mice used in this study also shared lupus-prone and synovitis-prone genetic backgrounds with MRL/lpr mice to varied extents. Previous studies have shown some MRL alleles significantly linked to the onset of spontaneous synovitis in the *lpr* constraint.[8 9] Therefore, there is a reason for the onset of synovitis in MCF_2 mice. This study showed the onset of synovitis in MCF_2 mice, although inflammation and erosive changes were present to a lesser extent than those in the original MRL/lpr mice. We thought that this was a countereffect of ankylosis on synovitis; however, this notion turned out to be erroneous. This may be partly due to the difference in bleeding condition and genetic effects derived from the C3H/lpr strain. Our results totally revised these considerations and enforced a notion that proliferating enthesitis entail specific mechanisms for the development of ankylosis.

Our results suggest a susceptibility locus in the middle of chromosome 11. As the number of markers and samples were not sufficient to detect complex loci, some loci may have remained undetected. However, the detected locus has a major effect on the development of synovial proliferation. This locus contains several genes that are highly conserved in a particular interval of human chromosome 17. To date, a high-resolution linkage and association mapping study identified a susceptibility locus for rheumatoid arthritis in this region.[10] The central part of mouse chromosome 11 also contains several loci associated with experimental autoimmune encephalomyelitis,[11 12] collagen-induced arthritis[13] and proteoglycan-induced arthritis.[14] This region is noteworthy when considering the genetic predisposition of rheumatoid arthritis.

A previous study using a larger number of backcross mice prepared from the same parental strains of MRL/Mp and C3H/He indicated that the five linkage loci are associated with the onset of arthritis.[9] None of these loci overlap with the present linkage region. This discrepancy is possibly due to a difference in the mouse generation used (N_2 or F_2), a difference in the housing condition or a suppressive effect of the Y chromosome derived from C3H/lpr as discussed previously while purporting a possible reason for the onset of new cases of ankylosis.[5]

ACKNOWLEDGEMENTS

We thank Ms N Yamaki, Dr N Tanda and Dr H Umeda for technical assistance, Mrs N Fujisawa for secretarial assistance and Dr M Nose for critical comments.

Authors' affiliations

Ming-Cai Zhang*, Fumiko Date, Hiroshi Furukawa, Masao Ono, Department of Pathology, Tohoku University Graduate School of Medicine, Sendai, Miyagi, Japan
Shiro Mori*, Department of Oral Medicine and Surgery, Tohoku University Graduate School of Dentistry, Sendai, Miyagi, Japan

*These authors contributed equally to this work.

Funding: This study was supported by Grants-in-Aid for Scientific Research from the Ministry of Education, Science, Sports, and Culture of Japan to SM (number 15390607) and MO (number 16390113).

Competing interests: None.

Correspondence to: Dr Masao Ono, Department of Pathology, Tohoku University Graduate School of Medicine, 2-1 Seiryo, Aoba, Sendai, Miyagi 980-8575, Japan; onomasao@mail.tains.tohoku.ac.jp

Accepted 10 July 2006
Published Online First 25 July 2006

REFERENCES

1 **Nordling C**, Karlsson-Parra A, Jansson L, Holmdahl R, Klareskog L. Characterization of a spontaneously occurring arthritis in male DBA/1 mice. *Arthritis Rheum* 1992;**35**:717–22.
2 **Holmdahl R**, Jansson L, Andersson M, Jonsson R. Genetic, hormonal and behavioural influence on spontaneously developing arthritis in normal mice. *Clin Exp Immunol* 1992;**88**:467–72.
3 **Lories RJ**, Matthys P, de Vlam K, Derese I, Luyten FP. Ankylosing enthesitis, dactylitis, and onychoperiostitis in male DBA/1 mice: a model of psoriatic arthritis. *Ann Rheum Dis* 2004;**63**:595–8.
4 **Oishi H**, Miyazaki T, Mizuki S, Kamogawa J, Lu LM, Tsubaki T, *et al*. Accelerating effect of an MRL gene locus on the severity and onset of arthropathy in DBA/1 mice. *Arthritis Rheum* 2005;**52**:959–66.
5 **Mori S**, Zhang MC, Tanda N, Date F, Nose M, Furukawa H, *et al*. Genetic characterization of spontaneous ankylosing arthropathy with unique inheritance from Fas-deficient strains of mice. *Ann Rheum Dis* 2006;**28**:1273–8.
6 **Komori H**, Furukawa H, Mori S, Ito MR, Terada M, Zhang MC, *et al*. A signal adaptor SLAM-associated protein regulates spontaneous autoimmunity and Fas-dependent lymphoproliferation in MRL-*Fas*^{lpr} lupus mice. *J Immunol* 2006;**176**:395–400.
7 **Lander E**, Kruglyak L. Genetic dissection of complex traits: guidelines for interpreting and reporting linkage results. *Nat Genet* 1995;**11**:241–7.
8 **Hang L**, Theofilopoulos AN, Dixon FJ. A spontaneous rheumatoid arthritis-like disease in MRL/l mice. *J Exp Med* 1982;**155**:1690–701.
9 **Kamogawa J**, Terada M, Mizuki S, Nishihara M, Yamamoto H, Mori S, *et al*. Arthritis in MRL/lpr mice is under the control of multiple gene loci with an allelic combination derived from the original inbred strains. *Arthritis Rheum* 2002;**46**:1067–74.
10 **Barton A**, Eyre S, Myerscough A, Brintnell B, Ward D, Ollier WE, *et al*. High resolution linkage and association mapping identifies a novel rheumatoid

arthritis susceptibility locus homologous to one linked to two rat models of inflammatory arthritis. *Hum Mol Genet* 2001;**10**:1901–6.
11 **Karlsson J**, Zhao X, Lonskaya I, Neptin M, Holmdahl R, Andersson A. Novel quantitative trait loci controlling development of experimental autoimmune encephalomyelitis and proportion of lymphocyte subpopulations. *J Immunol* 2003;**170**:1019–26.
12 **Butterfield RJ**, Blankenhorn EP, Roper RJ, Zachary JF, Doerge RW, Teuscher C. Identification of genetic loci controlling the characteristics and severity of brain and spinal cord lesions in experimental allergic encephalomyelitis. *Am J Pathol* 2000;**157**:637–45.
13 **Liljander M**, Sallstrom MA, Andersson S, Andersson A, Holmdahl R, Mattsson R. Identification of collagen-induced arthritis loci in aged multiparous female mice. *Arthritis Res Ther* 2006;**8**:R45.
14 **Adarichev VA**, Nesterovitch AB, Bardos T, Biesczat D, Chandrasekaran R, Vermes C, *et al*. Sex effect on clinical and immunologic quantitative trait loci in a murine model of rheumatoid arthritis. *Arthritis Rheum* 2003;**48**:1708–20.

APMIS 115: 1350–6, 2007
Printed in Denmark . All rights reserved

ISSN 0903-4641

Persistent expression of an unproductive immunoglobulin heavy chain allele with D_H-J_H-γ configuration in peripheral tissues

MASAO ONO[1] and MASATO NOSE[2]

[1]Department of Pathology, Tohoku University Graduate School of Medicine, Sendai, and [2]Department of Pathology, Ehime University School of Medicine, Toon, Japan

Ono M, Nose M. Persistent expression of an unproductive immunoglobulin heavy chain allele with D_H-J_H-γ configuration in peripheral tissues. APMIS 2007;115:1350–6.

Genomic recombination events, including VDJ recombination (VDJR) and class-switch recombination (CSR), are indispensable for the adaptation and progression of the acquired immune system. These processes are completed by orderly, temporal onsets of the gene rearrangements along with B-cell differentiation. The presence of various premature transcripts of immunoglobulin heavy chain (IgH) alleles has been demonstrated during B-cell ontogeny. These include D_H-J_H (DJ)-μ, J_H-μ, and sterile transcripts of C_H. Since these transcripts can be detected during the onset of VDJR and CSR, their presence is believed to reflect a structural change in the genome, favoring VDJR and CSR. This report presents evidence of persistent DJ transcription and onset of CSR on an unproductive IgH allele in peripheral tissues. Nucleotide sequence analysis revealed that these transcripts showed DJ-γ (Dγ) configuration and that characteristics of the variable region were essentially the same as those of the DJ-μ transcript previously described. It was noted that the small intestine abundantly expresses Dγ transcripts with γ2b and γ1 isotypes of the IgH constant region. The present findings indicate the onset of CSR preceding V_H to DJ joining in an unproductive IgH allele of the peripheral B cell and the specificity for the gut-associated condition for B-cell differentiation in the small intestine.

Key words: B cell; immunoglobulin; class switching; VDJ rearrangement; DJ transcript.

Masao Ono, Department of Pathology, Tohoku University Graduate School of Medicine, 2-1 Seiryo, Aoba-ku, Sendai, Miyagi 980-8575, Japan. e-mail: onomasao@mail.tains.tohoku.ac.jp

An immunoglobulin (Ig) heavy chain (IgH) gene consists of heterogeneous gene segments that separately code the four parts of IgH protein: the variable segment (V_H), diversity segment (D_H), junction segment (J_H), and constant region (C_H). Assemblies of V_H, D_H, and J_H segments, referred to as VDJ recombination (VDJR), necessarily occur during B-cell development in bone marrow and consequently form a continuous coding exon for the IgH-variable region (1). VDJR is an essential process for the acquisition of a broad range of structural variations of IgH that enable adaptive immune recognition of various pathogens. With the progression of the immune response, a subsequent process known as class-switch recombination (CSR) occurs in peripheral tissues (2–5) and changes an isotype of C_H, resulting in alteration of the effector functions of Ig. Disorders associated with defective CSR usually cause immune insufficiency in humans and mice (6–12); therefore, CSR is indispensable for normal development of the humoral immune response.

IgH gene alleles express germ line transcripts during B-cell differentiation, including JH-μ

Received 12 June 2007.
Accepted 2 July 2007.

(13), D_H-J_H (DJ)-μ (Dμ) (14) and sterile C_H transcripts (15–19). Although none of these transcripts exerts an effector function as an antibody, these are detected before or during the onset of VDJR and CSR in B-lineage cells. It has been proposed that these sterile transcripts participate in the formation of the structure of the IgH gene accessible for the factors involved in VDJR and CSR as well as the transcriptional regulators for these transcriptions.

We had previously searched for the nucleotide sequences of IgH transcripts of mouse hybridoma clones isolated from MRL/lpr, which was an autoimmune-prone strain of mice due to the defect in the apoptosis receptor gene—Fas (20, 21). In this study we identified an aberrant IgH transcript that represented a truncated variable region—DJ—with γ3 isotype of C_H (unpublished data). This finding suggested the presence of the DJ-γ (Dγ) transcript in the spleen of an MRL/lpr strain. Here we tested whether this aberrant transcript was expressed in peripheral tissues and in an autoimmune-dependent and/or a Fas-dependent fashion. The results provide the first evidence for the persistent expression of Dγ transcripts in mouse peripheral tissues. The present findings showed the fate of unproductive IgH alleles in peripheral environments and characteristics of IgH alleles associated with a specific immunological nature of the small intestine.

MATERIALS AND METHODS

Mice

MRL/Mp.*Fas*^{lpr} (MRL/lpr), C57BL/6.*Fas*^{lpr} (B6/lpr), and MRL/MpJ (MRL/+) strains of mice were obtained from the Jackson Laboratory (Bar Harbor, ME). C.B-17/Icr-scid/scid (SCID) mice were kindly donated by Dr. S. Ikehara (Kansai Medical University, Osaka, Japan). All mice were bred under specific pathogen-free conditions at the Institute for Animal Experimentation, Tohoku University, Sendai, Japan. The Tohoku University guidelines for animal experimentation were observed.

RNA preparation and analysis

Total RNA was prepared from thymus, spleen, axillary lymph nodes, mesenteric lymph node, peritoneal resident cells, small intestine with Peyer's patches, and bone marrow cells according to the regular protocol for Trisol™ agent (Invitrogen, Carlsbad, CA). Total RNA (20 μg) was denatured, electrophoresed in 1.2% agarose gel, and transferred onto a nylon membrane (BioRad, Tokyo, Japan) by the capillary transfer method. A hybridization probe (D_{SP2} probe, 78 nucleotide length) for the detection of DJ transcripts was prepared from a cloned cDNA containing the 5'-flanking sequence of the $D_{SP2.2}$ gene in pBluescript KS+ vector, which was obtained from the hybridoma 8H8 clone by reverse transcription-polymerase chain reaction (RT-PCR) with $D_{SP2.2}$ specific primers: D_{SP2}F1, 5'-ACTCTGCACTGCTACC-TCTGG-3', and D_{SP2}R1, 5'-GACAAAAATCCCT-GCCAAGTAAGG-3' (Fig. 1). It is known that the sequence of this amplified region is highly conserved among all members of the D_{SP2} family. Radioisotope labeling with [α^{32}P] dCTP was achieved by DNA polymerase reaction in the presence of the $D_{SP2.2}$ specific primers and 25 ng of the probe DNA. Hybridizations and washes were performed as described previously (22). The washed membrane was exposed to a high-sensitive film (Kodac X-OMAT AR) for 2 weeks.

RT-PCR and identification of the IgG subclass

Single-strand cDNA was prepared from 2 μg of total RNA with oligo-dT primers (50 pmol) and reverse transcriptase (200 U) derived from Moloney murine leukemia virus (Invitrogen). In RT-PCR, $V_{H\ BACK}$: AGGT[C,G][C,A]A[G,A]CTGCAG[C,G]AG-TC[T,A]GG (23), or D_{SP2}F2, TTACTTGGCAGG-GATTTTTG, and [^{32}P] 5'-end-labeled Cγ32, 5'-TGCATTTGAACTCCTTGCC-3', which is commonly present in all mouse IgG subclasses, were used to amplify V_H-D_H-J_H (VDJ)-γ or Dγ transcripts, respectively. The sequences of $V_{H\ BACK}$ and D_{SP2}F2 are known to be commonly present in the $V_{H\ J558}$ family genes and D_{SP2} family genes, respectively. The expression profile of IgG subclasses was determined by RT-PCR followed by digestions with *Bam* HI and *Xba* I endonucleases (22) (Fig. 3A).

Nucleotide sequencing

The RT-PCR products amplified with D_{SP2}F2 and Cγ32 (non RI-labeled) were phosphorylated by nucleotide kinase reaction and cloned into a pBluescript

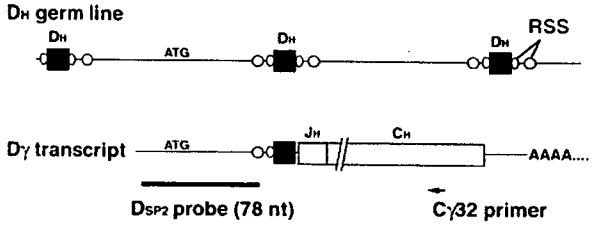

Fig. 1. Hybridization probe to detect DJ transcripts in Northern hybidization analysis. The probe fragment corresponds to the 5' flanking sequence of the $D_{SP2.2}$ gene. *RSS*, recombination signal sequence; D_H, a coding segment for the diversity segment of IgH; ATG, initiation codon; nt, nucleotide length.

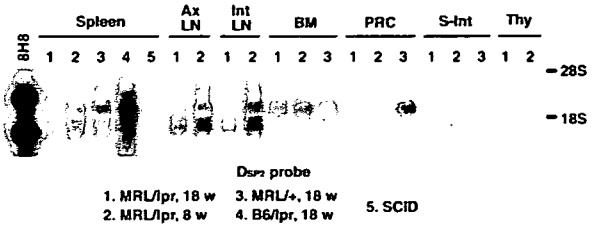

Fig. 2. Expression of DJ transcripts *in vivo*. Total RNA samples (20 μg/lane) prepared from indicated various organs or a cell type were analyzed with Northern hybridization using the ^{32}P-labeled D_{SP2} probe as shown in Fig. 1. The lower molecular weight signal of 8H8 corresponds to the Dγ3 transcript. *Ax LN*, axillary lymph node; *Int LN*, intestinal lymph node; *BM*, bone marrow; *PRC*, peritoneal resident cells; *S-Int*, small intestine; *Thy*, thymus; *18S*, ribosomal RNA 18 S; *28S*, ribosomal RNA 28S; SCID, severe combined immunodeficiency strain of mice.

KS+ vector. Nucleotide sequences in randomly selected clones were determined by dideoxy termination reactions.

RESULTS

Expression of DJ transcripts in peripheral tissues

We performed Northern hybridization with the D_{SP2} probe (Fig. 1) to show the presence of premature IgH transcripts containing the 5′ flanking sequence of the D_{SP2} family genes and, if present, their specificity to the autoimmune onset in MRL/lpr mice. Total RNA samples were prepared from various immune tissues of mice, including 8- and 18-week-old mice, as controls of pre-diseased and diseased conditions, respectively (Fig. 2). It was of particular note that specific signals appeared in heterogeneous and tissue-specific patterns. The spleen, axillary lymph node, and mesenteric lymph node expressed at least three different transcripts. In comparison, the bone marrow, peritoneal resident cells, and small intestine showed simpler patterns; the bone marrow and peritoneal resident cells expressed longer transcripts, while the small intestine expressed shorter transcripts. No signal was detected in the spleen of SCID mice, which lack both B and T cells due to the genetic defect in VDJR. This finding indicates high specificity of the D_{SP2} probe in detection of the transcripts containing the 5′ flanking region of the D_{SP2} family genes.

A previously isolated hybridoma clone, namely 8H8, was also analyzed as a reference for the Dγ transcript in this study. This hybridoma clone was established from the spleen of an autoimmune-prone strain MRL/lpr. A sequencing analysis of 8H8 revealed the expression of an aberrant transcript with Dγ configuration that contained the 5′ flanking region of the $D_{SP2.2}$ gene segment (data not shown). These findings had suggested that the *lpr* mutation, which is known to cause the defect in the apoptosis-related receptor Fas and the onset of autoimmune diseases, also caused the pathological expression of such aberrant transcripts. Our present findings did not support this possibility because no distinct signal was observed for the MRL/lpr preparations.

Identification and characterization of IgG-class-switched DJ transcripts

The presence of the longer transcripts was demonstrated in various immune tissues as well as the bone marrow except the small intestine (Fig. 2). It seemed reasonable to consider that the longer transcripts were Dμ because past studies had shown the presence of Dμ in the bone marrow. On the other hand, the shorter transcripts remained to be elucidated. A further suggestion respecting this issue arose from the demonstration of shorter transcripts in 8H8, which is a mouse hybridoma shown to express a Dγ transcript. Therefore, we attempted to amplify Dγ transcripts in the spleen and small intestine by RT-PCR. Using the consensus primers D_{SP2}F2 and Cγ32 (Fig. 3A), we obtained the amplification for cDNA prepared from the spleen and small intestine, and succeeded in cloning them in plasmid vectors. 100 clones were randomly isolated for each tissue and analyzed further. Of these, 38 spleen-derived and 18 small intestine-derived clones were found to harbor insert fragments with a Dγ configuration. Excluding repeatedly appearing clones recognized by sequence identity, 17 spleen-derived and 9 small intestine-derived clones were finally obtained as independent clones. Their sequence data demonstrated that the Dγ transcript in the spleen shared common characteristics with the Dμ transcript or DJ genomic fragment reported previously (23–26): under-representation of RF2 in the D_H segment (Dμ selection), presence of D_H-D_H joining, usage of $D_{H\ SP2.12}$ and $D_{H\ SP2.13}$ previously iden-

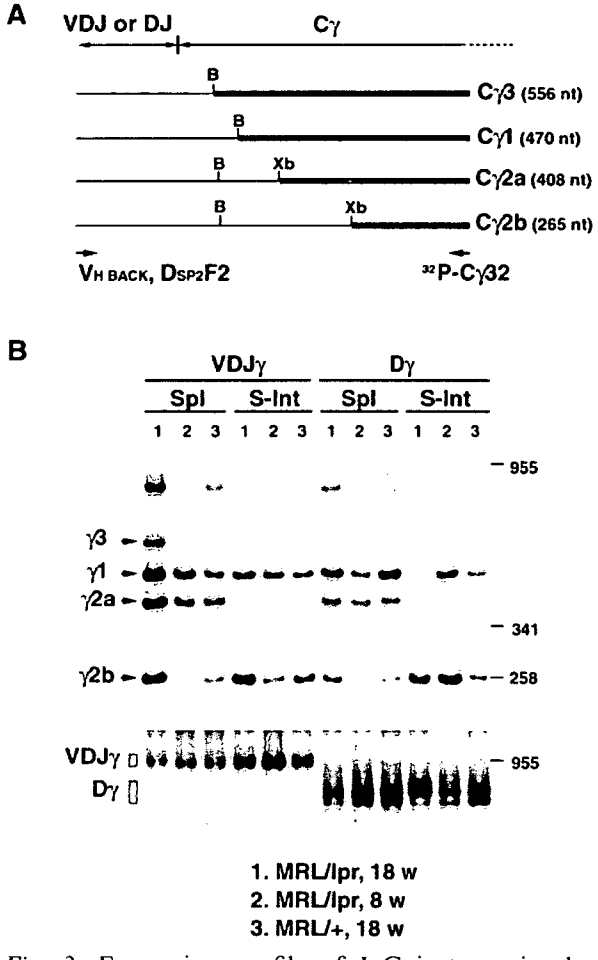

Fig. 3. Expression profile of IgG isotypes in the spleen and small intestine in MRL strains of mice. (A) Schematic representation of the differential detection of four IgG subclasses at an mRNA level. $V_{H\ BACK}$ or $D_{SP2}F2$ primer was used for the amplification of VDJ-γ or Dγ transcript, respectively. (B) *BamHI*; *Xb*, *XbaI*. *B*, IgG isotype profile of VDJ-γ and Dγ transcripts in the spleen and small intestine. A signal corresponding to each IgG isotype was indicated. Cγ; IgG constant region; Cγ3, IgG3 constant region; Cγ1, IgG1 constant region; Cγ2a, IgG2a constant region; Cγ2b, IgG2b constant region; *Spl*, spleen; *S-Int*, small intestine; nt, nucleotide length.

tified in MRL/lpr, and frequent N nucleotide insertions in the spleen of aged mice (Table 1). These characteristics were found to be largely true for the small intestine; however, lower frequencies of N insertions and RF1 usage in the small intestine than in the spleen are not precluded.

An isotype pattern of Dγ constant region was explored by the semi-quantitative method developed previously (22) (Fig. 3A). The results demonstrated a tissue- and age-specific isotype pattern of Dγ and VDJ-γ transcripts (Fig. 3B). Dγ and VDJ-γ transcripts in the small intestine represented a remarkable predominance of γ1 and γ2b isotypes in all mice examined. An aging-dependent relative increase in the expression of γ2b and γ3 of VDJ-γ and γ2b of Dγ was observed in the spleen of the MRL/lpr strain.

DISCUSSION

The present study provided the first evidence of the presence of Dγ transcripts in peripheral tissues. D_H to J_H joining followed by Dμ transcription readily takes place on both IgH alleles of a pro-B cell in the bone marrow. The subsequent joining, V_H to DJ, followed by activation of the V_H promoter on either allele achieves transcription for the production of the IgM heavy chain in the bone marrow, while, in a case where the transcription is productive for IgM, the other allele is no longer processed. This abortive allele is so far considered to be the origin of all DJ transcripts in the peripheral tissues.

Northern hybridization revealed that different kinds of DJ transcripts are present in the peripheral tissues. The expression level of these DJ transcripts seems to be so low that it has taken 2 weeks for the specific signal of the hybridized probe to be visible. However, the level of their peripheral expression is comparable to the bone marrow. Provided that bone marrow mainly produces Dμ transcripts, spleen, lymph node, thymus, and small intestine produce other types of DJ transcripts than Dμ. The present sequence data and RT-PCR-based isotyping data confirmed the presence of Dγ transcripts in the spleen and small intestine, indicating that the transcription and the onset of CSR occur on unproductive IgH alleles in peripheral tissues. Although the biological significance of the peripheral expression of DJ transcripts remains unclear, these findings provide new insights into tissue specificity in peripheral B-cell differentiation or the mechanism for B- cell receptor editing in peripheral tissues.

Dμ transcripts harbor a leader peptide sequence in the 5′-region. Therefore, Dμ transcripts with a particular reading frame—RF2—can be translated into a cell surface protein con-

TABLE 1. *Characteristics of Dγ transcripts in the spleen and small intestine of an MRL/lpr mouse*[1)]

Clone ID	DH sequence	N/P sequence	JH sequence	J_H[2)]	C_H	D_H[3)]
I. Spleen						
S16	TC TAC TAT GGT GAC TAC	GGC GGA	TTT GCT TAC TGG	3	γ2a	2.13
S17-1	CC TAC TAT AGT AAC TAC	GTG GG	T GCT ATG GAC TAC TGG	4	γ3	2.x
S17-2	CC TAC TAT AGT AAC TAC TTA CGA	GGG ATT	TTT GCT TAC TGG	3	γ3	2.x+2.2
S36	CC TAC TAT AGT AAC TAC	GTT TG	T GCT ATG GAC TAC TGG	4	γ1	2.x
S39	CC TAC TAT AGT TAC TAT AGT TAC G		CC TGG TTT GCT TAC TGG	3	γ2a	2.12
S65	CC TAC TAT AGT AAC T		GG TTT GCT TAC TGG	3	γ1	2.x
S70	CC TAC TAT AGT TAC T		CC TGG TTT GCT TAC TGG	3	γ1	2.12
S9	CC TA	A GG	T GCT ATG GAC TAC TGG	4	γ2a	2.10,12, or x
S77	TCT ATG ATG GTT ACT A	AA CC	C TGG any	γ1	2.9	
S8	CCT ACT ATA GTT ACT ATA GTT ACG AC	G T	AC TAC TTT GAC TAC TGG	2	γ2b	2.12
S11	C CTA CTA TAG TAA CT	T TCT	TTT GCT TAC TGG	3	γ2b	2.x
S33	C CTA CTA TAG TTA CTA TAG TTA CG	G AAC TCC T	AT TAC TAT GCT ATG GAC TAC TGG	4	γ2b	2.12
S37[5)]	C CTA CTA TAG TAA C	CG AGG	GCT TAC TGG	3	γ1	2.x
S38	T CTA CTA TGG TGA CT	T TTT	TAT GCT ATG GAC TAC TGG	4	γ3	2.13
S43	C CTA CTA TAG TAA C	CG AGG	GCT TAC TGG	3	γ2a	2.x
S63	T CTA CTA	CCC A	AC TGG any	γ2b	2.2, 5, or 13	
S7	C CTA CTA TAG TTA	GGG CGT	TTT GCT TAC TGG	3	γ2a	2.12
II. Small intestine						
I27	CCT ACT ATA GTA ACT AC	G TGA TGA	GAC TAC TGG	2 or 4	γ2b	2.x+2.9
I22	C CTA CTA TAC	GTA CGA	TTT GAC TAC TGG	2	γ2b	2.x+2.10
I28	C CAA CTA TAG TAA	TTT TT	C TAT GTT ATG GAC TAC TGG	4	γ2b	2.x
I32	C CTA CTA TA		T GTT ATG GAC TAC TGG	4	γ2b	2.x, 10, or 12
I51	C CTA CTA TAG TA		C TAT GTT ATG GAC TAC TGG	4	γ2b	2.x
I57[6)]	C CTA CTA		GGG TTT TCT TAC TGG	3	γ1	2.x, 10, or 12
I71	C CTA CTA		GGG TTT TCT TAC TGG	3	γ2b	2.x, 10, or 12
I74	T CTA TGA TGG TTA CTA C		AT GTT ATG GAC TAC TGG	4	γ2b	2.9
I75	C CTA CTA TAG TAA C	CT CGG AGG	GTT ATG GAC TAC TGG	4	γ2b	2.x

[1)] We used cDNA derived from a 20-week-old male MRL/lpr mouse for this sequence analysis. A residue of mutation is underlined.
[2)] A JH family designation was determined according to the genomic sequence of C57BL/6 in the public data base.
[3)] A DH SP2 family designation was determined according to the genomic sequences in the public data base (Accession number: J00431, J00432, J00433, J00435, J00437, J00438 or in previous reports (Kaartinen & Mekela, 1985, Feeney, 1990, Gu et al., 1991, Kompfner et al., 2001).
[4)] A RF was determined by the numbering system proposed in a previous report.
[5)] S37 is a γ isotype-switching variant of S43.
[6)] I57 is a γ isotype-switching variant of I71.

taining an IgM constant region (14). Although the rationale underlying the expression of the Dμ protein is not completely elucidated, it has been shown that the RF2 usage in Dμ transcripts is under-represented in B-lineage cells but not in T-lineage cells, which, however, in part, undergo DJ joining in conjunction with T-cell receptor (TCR) rearrangement (24). It is proposed that the Dμ protein physiologically mediates signals for the elimination of pro-B cells in the bone marrow. The present study has shown the under-representation of RF2 usage for Dγ transcripts in the spleen and small intestine, as previously demonstrated for Dμ transcripts in the bone marrow. This finding indicates that the cells producing Dγ transcripts in the peripheral tissues have undergone Dμ selection in the bone marrow; therefore, they are B-lineage cells. The frequent usage of RF3 was noted for the Dγ transcripts in the small intestine. This should be confirmed by further sequence analyses.

The findings on VDJ-γ and Dγ isotype pattern of IgG constant regions clearly indicate selective expression of γ2b and, to a lesser extent, γ1 of C_H in the small intestine. The different isotype pattern was observed in the spleen in the same individual (Fig. 3B). This may suggest that the tissue-specific environment controls the onset of CSR in peripheral B cells. Intestinal mucosa is known to present a specific condition for B cells that favors CSR to α isotype of C_H (27–29). Transforming growth factor-β (TGF-β) has been shown to deliver a gut-associated signal through TGF-β receptor 2 (30). Past studies have shown that TGF-β facilitates CSR to IgG2b as well as IgA at the culture level (31, 32). The over-representation of IgG2b subclass in the small intestine may be associated with the gut-associated condition. In addition, it is noted that both productive and unproductive alleles of IgH present a similar isotype pattern in the spleen and small intestine. This sug-

gests that the two IgH alleles are under the same regulation for CSR.

Our preliminary finding from a 8H8 hybridoma clone isolated from an autoimmune-prone strain of mice—MRL/lpr—provides insight into the association of Dγ transcripts with an autoimmune mechanism. The present study has shown that the Dγ transcripts derived from MRL/lpr do not represent a specific pattern in the IgH isotype distribution in the spleen and small intestine. The nucleotide sequence data confirmed that the forbidden RF usage in Dμ transcript in bone marrow—RF2—was not activated in association with the autoimmune onset in aged MRL/lpr, further suggesting that Fas is not involved in the elimination of RF2 usage in B cells in peripheral tissues. The relative increase of γ3 isotype in the spleen of aged MRL/lpr was also noted in the present study. This confirms our previous finding of high expression of IgG3 in aged MRL/lpr (33). IgG3 is specifically induced in mice by bacterial antigens, i.e., lipopolysaccharide, and has long been considered the disease-associated antibody subclass in this strain. Small intestine has been thought to be a responsible organ where IgG3 is produced in response to antigens of commensal bacteria in this strain; however, the present results confute this idea. The role of Dγ transcription in physiological and pathological B-cell development remains to be elucidated.

The authors thank Tokuo Yamamoto for critical discussion and Noriko Fujisawa for secretarial assistance. This study was supported by Grants-in-Aid for Scientific Research from the Ministry of Education, Science, Sports, and Culture of Japan to MO (No. 16390113).

REFERENCES

1. Hozumi N, Tonegawa S. Evidence for somatic rearrangement of immunoglobulin genes coding for variable and constant regions. Proc Natl Acad Sci USA 1976;73:3628–32.
2. Honjo T, Kataoka T. Organization of immunoglobulin heavy chain genes and allelic deletion model. Proc Natl Acad Sci USA 1978;75:2140–4.
3. Seidman JG, Leder P. The arrangement and rearrangement of antibody genes. Nature 1978;276:790–5.
4. Kataoka T, Kawakami T, Takahashi N, Honjo T. Rearrangement of immunoglobulin gamma 1-chain gene and mechanism for heavy-chain class switch. Proc Natl Acad Sci USA 1980;77:919–23.
5. Davis MM, Calame K, Early PW, Livant DL, Joho R, Weissman IL, et al. An immunoglobulin heavy-chain gene is formed by at least two recombinational events. Nature 1980;283:733–9.
6. Allen RC, Armitage RJ, Conley ME, Rosenblatt H, Jenkins NA, Copeland NG, et al. CD40 ligand gene defects responsible for X-linked hyper-IgM syndrome. Science 1993;259:990–3.
7. DiSanto JP, Bonnefoy JY, Gauchat JF, Fischer A, de Saint Basile G. CD40 ligand mutations in x-linked immunodeficiency with hyper-IgM. Nature 1993;361:541–3.
8. Aruffo A, Farrington M, Hollenbaugh D, Li X, Milatovich A, Nonoyama S, et al. The CD40 ligand, gp39, is defective in activated T cells from patients with X-linked hyper-IgM syndrome. Cell 1993;72:291–300.
9. Muramatsu M, Kinoshita K, Fagarasan S, Yamada S, Shinkai Y, Honjo T. Class switch recombination and hypermutation require activation-induced cytidine deaminase (AID), a potential RNA editing enzyme. Cell 2000;102:553–63.
10. Revy P, Muto T, Levy Y, Geissmann F, Plebani A, Sanal O, et al. Activation-induced cytidine deaminase (AID) deficiency causes the autosomal recessive form of the Hyper-IgM syndrome (HIGM2). Cell 2000;102:565–75.
11. Imai K, Catalan N, Plebani A, Marodi L, Sanal O, Kumaki S, et al. Hyper-IgM syndrome type 4 with a B lymphocyte-intrinsic selective deficiency in Ig class-switch recombination. J Clin Invest 2003;112:136–42.
12. Al-Alem U, Li C, Forey N, Relouzat F, Fondanèche MC, Tavtigian SV, et al. Impaired Ig class switch in mice deficient for the X-linked lymphoproliferative disease gene Sap. Blood 2005;106:2069–75.
13. Thompson A, Timmers E, Schuurman RK, Hendriks RW. Immunoglobulin heavy chain germ-line JH-C mu transcription in human precursor B lymphocytes initiates in a unique region upstream of DQ52. Eur J Immunol 1995;25:257–61.
14. Reth MG, Alt FW. Novel immunoglobulin heavy chains are produced from DJH gene segment rearrangements in lymphoid cells. Nature 1984;312:418–23.
15. Alt FW, Rosenberg N, Enea V, Siden E, Baltimore D. Multiple immunoglobulin heavy-chain gene transcripts in Abelson murine leukemia virus-transformed lymphoid cell lines. Mol Cell Biol 1982;2:386–400.
16. Berton MT, Uhr JW, Vitetta ES. Synthesis of germ-line gamma 1 immunoglobulin heavy-chain transcripts in resting B cells: induction by interleukin 4 and inhibition by interferon gamma. Proc Natl Acad Sci USA 1989;86:2829–33.
17. Lutzker S, Rothman P, Pollock R, Coffman R, Alt

FW. Mitogen- and IL-4-regulated expression of germ-line Ig gamma 2b transcripts: evidence for directed heavy chain class switching. Cell 1988;53: 177–84.
18. Stavnezer J, Radcliffe G, Lin YC, Nietupski J, Berggren L, Sitia R, et al. Immunoglobulin heavy-chain switching may be directed by prior induction of transcripts from constant-region genes. Proc Natl Acad Sci USA 1988;85:7704–8.
19. Lebman DA, Nomura DY, Coffman RL, Lee FD. Molecular characterization of germ-line immunoglobulin A transcripts produced during transforming growth factor type beta-induced isotype switching. Proc Natl Acad Sci USA 1990;87:3962–6.
20. Takahashi S, Itoh J, Nose M, Ono M, Yamamoto T, Kyogoku M. Cloning and cDNA sequence analysis of nephritogenic monoclonal antibodies derived from an MRL/lpr lupus mouse. Mol Immunol 1993;30:177–82.
21. Ono M, Yamamoto T, Kyogoku M, Nose M. Sequence analysis of the germ-line VH gene corresponding to a nephritogenic antibody in MRL/lpr lupus mice. Clin Exp Immunol 1995;100:284–90.
22. Ono M, Yamamoto T, Nose M. A simple method based on PCR for detecting the relative mRNA amounts of the four mouse IgG subclasses. J Immunol Methods 1995;184:63–9.
23. Kaartinen M, Makela O. Reading of D genes in variable frames as a source of antibody diversity. Immunol Today 1985;6:324–27.
24. Gu H, Kitamura D, Rajewsky K. B cell development regulated by gene rearrangement: arrest of maturation by membrane-bound D mu protein and selection of DH-element reading frames. Cell 1991;65:47–54.
25. Kompfner E, Oliveira P, Montalbano A, Feeney AJ. Unusual germline DSP2 gene accounts for all apparent V-D-D-J rearrangements in newborn, but not adult, MRL mice. J Immunol 2001;167: 6933–8.
26. Feeney AJ. Lack of N regions in fetal and neonatal mouse immunoglobulin V-D-J junctional sequences. J Exp Med 1990;172:1377–90.
27. Macpherson AJ, Gatto D, Sainsbury E, Harriman GR, Hengartner H, Zinkernagel RM. A primitive T cell-independent mechanism of intestinal mucosal IgA responses to commensal bacteria. Science 2000;288:2222–6.
28. Macpherson AJ, Lamarre A, McCoy K, Harriman GR, Odermatt B, Dougan G, et al. IgA production without mu or delta chain expression in developing B cells. Nat Immunol 2001;2:625–31.
29. Fagarasan S, Kinoshita K, Muramatsu M, Ikuta K, Honjo T. In situ class switching and differentiation to IgA-producing cells in the gut lamina propria. Nature 2001;413:639–43.
30. Cazac BB, Roes J. TGF-beta receptor controls B cell responsiveness and induction of IgA in vivo. Immunity 2000;13:443–51.
31. Iwasato T, Arakawa H, Shimizu A, Honjo T, Yamagishi H. Biased distribution of recombination sites within S regions upon immunoglobulin class switch recombination induced by transforming growth factor beta and lipopolysaccharide. J Exp Med 1992;175:1539–46.
32. Park SR, Seo GY, Choi AJ, Stavnezer J, Kim PH. Analysis of transforming growth factor-beta1-induced Ig germ-line gamma2b transcription and its implication for IgA isotype switching. Eur J Immunol 2005;35:946–56.
33. Takahashi S, Nose M, Sasaki J, Yamamoto T, Kyogoku M. IgG3 production in MRL/lpr mice is responsible for development of lupus nephritis. J Immunol 1991;147:515–9.

Tetsuya KODAMA

差出人: BBA - Biomembranes (ELS) [bbamem@elsevier.com]
送信日時: 2008年3月13日木曜日 1:21
宛先: koshiyama@me.es.osaka-u.ac.jp
件名: BBAMEM-07-460R1: Final Decision

Manuscript No.: BBAMEM-07-460R1
Title: Molecular Dynamics Simulation of Structural Changes of Lipid Bilayers Induced by Shock Waves: Effects of Incident Angles Article Type: Regular Paper BBA Section: BBA - Biomembranes Corresponding Author: Dr. Kenichiro Koshiyama All Authors: Kenichiro Koshiyama, Ph.D.; Tetsuya Kodama, Ph.D.; Takeru Yano, Ph.D.; Shigeo Fujikawa, Doctor of engineering Submit Date: Nov 12, 2007

Dear Dr. Koshiyama:

We are pleased to inform you that the above-noted paper has been accepted for publication in Biochimica et Biophysica Acta - Biomembranes.

Your article will be published rapidly in electronic form, as well as in the traditional print journal in the first available scheduled issue.

Shortly, you will receive an acknowledgement letter detailing information regarding proofs, reprints and copyright transfer.

We once again thank you for your contribution to BBA - Biomembranes and hope that you will continue to submit your research articles to the journal.

Yours sincerely,

Dr. Jean-Marie Ruysschaert
Executive Editor
BBA - Biomembranes

Molecular Dynamics Simulation of Structural Changes of Lipid Bilayers Induced by Shock Waves: Effects of Incident Angles

Kenichiro Koshiyama[a]*, Tetsuya Kodama[b], Takeru Yano[c], and Shigeo Fujikawa[d]

[a] Graduate School of Engineering Science, Osaka University, Toyonaka, 560-8531, Japan

[b] Graduate School of Biomedical Engineering, Tohoku University, Sendai, 980-8575, Japan

[c] Graduate School of Engineering, Osaka University, Suita, 565-0871, Japan

[d] Graduate School of Engineering, Hokkaido University, Sapporo, 060-8628, Japan

Key words: acoustic wave; cell membrane permeabilization; impulse; shear force; sonoporation; ultrasound

* Corresponding author

Address: Department of Mechanical Science & Bioengineering, Graduate School of Engineering Science, Osaka University, Toyonaka, 560-8531, Japan

Tel.:+81(6)6850-6173

Fax:+81(6)6850-6172

E-mail: koshiyama@me.es.osaka-u.ac.jp

Summary

The effects of incident angles of shock waves on the structural changes of a lipid bilayer at the molecular level have been examined using unsteady and nonequilibrium molecular dynamics simulations. We found that the half of the bilayer directly exposed to shock waves is sensitive to an incident shock wave; therefore, the lateral displacement and the tilts of lipid molecules are enhanced with an increase in the incident shock angle. On the other hand, the other half of the bilayer is found to be insensitive to the change in the incident shock angle. This difference in the sensitivity to the incident shock wave results in the fact that only the normal component of the applied oblique impulse of the shock wave is transferred across the bilayer. This also suggests that the irradiation by shock waves may induce a jet-like streaming of the cytoplasm toward the nucleus.

Abstract

Unsteady and nonequilibrium molecular dynamics simulations of the response of dipalmitoylphosphatidylcholine (DPPC) bilayers to the shock waves of various incident angles are presented. The action of an incident shock wave is modeled by adding a momentum in an oblique direction to water molecules adjacent to a bilayer. We thereby elucidate the effects of incident shock angles on (i) collapse and rebound of the bilayer, (ii) lateral displacement of headgroups, (iii) tilts of lipid molecules, (iv) water penetration into the hydrophobic region of the bilayer, and (v) momentum transfer across the bilayer. The number of water molecules delivered into the hydrophobic region is found to be insensitive to incident shock angles. The most important structural changes are the lateral displacement of headgroups and tilts of lipid molecules, which are observed only in the half of the bilayer directly exposed to a shock wave for all incident shock angles studied here. As a result, only the normal component of the added oblique momentum is substantially transferred across the bilayer. This also suggests that the irradiation by shock waves may induce a jet-like streaming of the cytoplasm toward the nucleus.

1. Introduction

The cell membrane permeabilization technique utilizing mechanical forces due to high-intensity acoustic waves (shock wave or ultrasound) is a promising method of noninvasive drug and gene delivery into the cytoplasm [1-5]. For the last decade, several authors have addressed the permeabilization mechanisms, in vitro and in vivo, which are fundamentals for the complete development of drug and gene delivery methods based on shock waves or ultrasound [6-14]. They have reported that cavitation-induced nonthermal effects (e.g., radiation force, micro-streaming, micro-jets, or shock waves from cavitation bubbles) can induce reversible lesions of cell membranes, and the cell membranes are thereafter permeabilized [6-14].

The above mentioned studies are limited to the macroscopic or cellular level. At the microscopic or molecular level, on the other hand, the mechanisms of the permeabilization induced by shock waves or ultrasound are not well understood. Recently, we conducted molecular dynamics (MD) simulations of the structural changes of phospholipid bilayers of cell membranes induced by the action of shock waves [15]. One of the important findings was that the resulting collapse and rebound of a bilayer are followed by the penetration of water molecules into the hydrophobic region of the bilayer.

In the simulations, the propagation direction of the applied incident shock waves was parallel to the bilayer normal direction. However, bilayers are generally undulating on a length scale well beyond their thickness [16]. That is, the incident shock angles on the membrane surface practically vary with the location on the surface where the shock wave impacts. Furthermore, a numerical analysis in fluid dynamics [17] points out that an oblique impact of a shock wave induces a kind of shear flow around cell membranes and the forces resulting from the flow field are responsible for cell deformation and lysis. The effects of the incident shock angles on the structural changes of a lipid bilayer underlie the permeabilization mechanisms at the molecular level. Therefore, the objective of this study is to analyze the structural changes of a lipid bilayer by using the shock waves of various incident shock angles.

The foundation of all biological membranes is the lipid bilayer structure consisting of two leaflets of phospholipids. Thus, their dynamics (i.e., rearrangement of the phospholipids) is central to understanding the behavior of biological membranes. MD simulations of lipid bilayers have provided accurate models of biological membranes at the nanometer and nanosecond scales [18-21], and the molecular behaviors of lipids, water, and membrane proteins in equilibrium states have been clarified[18, 22-25]. Moreover, the

studies on the lipid bilayer responses to surface area changes [26], mechanical stresses [27], electric fields [28-30], and shear flows [31-33] are beginning to be conducted.

However, these studies involve responses in the steady or almost steady states. We emphasize that a shock wave is a high-pressure wave with a steep wave front that propagates at a supersonic speed, and it passes the cell membrane within a very short time of the order of picoseconds. Therefore, understanding the high-speed phenomenon induced by the interaction of a shock wave with a lipid bilayer should be indispensable. We address the lipid bilayer responses not to steady but unsteady actions induced by shock waves, particularly focusing on the effect of various incident shock angles.

In the previous study [15], we have modeled a shock wave by its impulse and performed unsteady and nonequilibrium MD simulations. Here, we slightly modify the shock wave impulse model to take account of incident shock angles, and the modified model is described in the Methods section. In the Results section, the collapse stage and the rebound stage are defined, and then the lateral displacement of headgroups, tilts of lipid molecules, water penetration into the hydrophobic region of a bilayer, and the momentum transfer across the bilayer are analyzed in detail. We finally summarize the effects of incident shock angles on the structural changes of a bilayer and discuss possible streaming in the cytoplasm induced by shock waves in the Summary and discussion section.

2. Methods

2.1. Lipid bilayer system

In this study, we investigated the effect of the incident angle of a shock wave on a lipid bilayer distributed on a plane surface (see Fig. 1). The lipid bilayer system comprised 128 DPPC molecules fully hydrated by 16455 water molecules. For equilibration, we performed 20-ns simulations with our force fields (see below) in a constant *NPT* ensemble, and we obtained the equilibrated bilayer system of volume $6.56\times6.40\times15.90$ nm^3, where the linear dimension of the simulation box in the z direction normal to the bilayer plane (the xy plane) is 15.90 nm. The detailed simulation procedures for the bilayer equilibration are summarized elsewhere [15, 19]. We remark that our system included a large water layer of thickness about 12 nm, whereas the thickness of the bilayer was about 4 nm. This is because this simulation of a shock wave required a large number of water molecules, as explained below.

The force fields for DPPC and water were consistent with those employed in the